Tellus (1990), *42A*, 413–428

Semi-Lagrangian moisture transport in the NMC spectral model

By DAVID L. WILLIAMSON*, *UCAR Visiting Scicentist Program, National Meteorological Center, World Weather Building, 5200 Auth Road, Washington, D.C. 20233 USA*

(Manuscript received 15 March 1989; in final form 12 July 1989)

ABSTRACT

The moisture advection component of the National Meteorological Center global spectral model is replaced with a semi-Lagrangian transport scheme. Several interpolation schemes, both monotonic and nonmonotonic, which were not eliminated from contention in earlier studies with simple test systems, are compared for moisture transport in five-day forecasts. The observed conservation properties of the schemes are considered first. Many of the schemes are found to be unsatisfactory with respect to conservation although several are very good. The best nonmonotonic interpolants are Hermite cubic and a rational cubic both coupled with a cubic derivative estimate. The best monotonic interpolants are these same two with the cubic derivative estimate modified to satisfy the appropriate C^0 monotonicity condition. The conservation aspects of these four schemes are better than the original spectral scheme if their computational sources are compared to the negative mixing ratios introduced by the spectral method. The skill of the semi-Lagrangian forecasts as measured by the traditional global skill scores (anomaly correlation and rms) is the same as that of the original spectral model. The characteristics of the precipitation in the semi-Lagrangian forecasts are very different from those of the spectral forecast. While the major precipitation events are similar in the two in both magnitude and location, the patterns of light precipitation are very different. The spectral model produces regions of light precipitation which are attributable to spectral truncation. The semi-Lagrangian method shows no similar spurious precipitation.

1. Introduction

The spectral transform method has proven to be excellent for calculating nonlinear, adiabatic fluid flow on the surface of a sphere. As a result, it has been adopted as the basis of many operational global numerical weather prediction models. The spectral approach, however, has serious deficiencies in physically representing the advection of water vapor, usually expressed as mixing ratio or specific humidity. The problem is most noticeable as regions of negative mixing ratio which are inconsistent with physical parameterizations as well as reality. Various computational fixes have been included in models to eliminate these negative regions (Mahlman and Sinclair, 1977; Royer, 1986); however, they result in significant computational sources or computational transport. Less noticeable, but equally serious, are regions of overshoot. Unlike negative mixing ratios, it is not obvious from the moisture field itself when overshooting has occurred, and thus it cannot be corrected or even monitored before the physical parameterizations are invoked. The overshoot can erroneously interact with the parameterizations to produce spurious precipitation. An example of such spurious precipitation is shown later in this paper.

Rasch and Williamson (1989) and Williamson years. Rasch and Williamson (1989) intermoisture transport approach to couple with global spectral transform nonlinear dynamical models. Their approach consists of semi-Lagrangian transport with shape preserving interpolation. Semi-Lagrangian transport is chosen because it has no stability condition restriction on the time step and thus does not suffer from the usual pole problem associated

* Permanent affiliation: National Center for Atmospheric Research, Box 3000, Boulder, CO 80307, USA; sponsored by the National Science Foundation.

with explicit gridpoint schemes nor from significant phase errors associated with implicit gridpoint schemes. Shape preserving denotes a class of interpolation methods that maintain certain properties suggested by the data. Such properties include monotonicity and convexity, and provide a means of avoiding the oscillations often seen in polynomial interpolation. These methods reduce or eliminate the overshooting possible with the semi-Lagrangian transport when polynomial interpolation is adopted.

A large number of shape preserving interpolants have been introduced in the past few years. Rasch and Williamson (1988) intercompared many of these schemes in terms of their accuracy in representing a variety of shapes which differed in their degree of continuity, monotonicity and convexity. Many of these interpolants were found to be less accurate or not more accurate but more complicated and expensive to implement than others. Those that fell into these less advantageous categories were eliminated from further consideration. The remaining, better schemes were then used within the semi-Lagrangian technique for the solution of one-dimensional uniform advection of prescribed initial shapes. These advective tests provided the basis for the elimination of some additional interpolants from further consideration.

The more attractive shape preserving schemes were applied to two-dimensional semi-Lagrangian advection in plane and spherical geometry by Williamson and Rasch (1989). These tests involved nondeformational advection of initially specified local structures. They demonstrated the viability of coupling shape-preserving interpolation with semi-Lagrangian transport in spherical geometry and again provided the basis for elimination of some of the schemes from further contention. However, these basic tests do not allow one to choose one scheme as best for a particular application such as moisture advection in a global forecast model. They do provide the basis of elimination of many of the schemes that have been introduced in the recent shape preserving literature. Only the few remaining schemes need be considered in the more complex problem at hand. This paper does just that by applying these schemes to moisture advection in forecasts with the National Meteorological Center (NMC) global spectral forecast model. Section 2 describes, in general terms, the original NMC model and the modifications made to incorporate semi-Lagrangian moisture advection. The various interpolation schemes are reviewed in Section 3. Detailed formulae are not included; rather references are made to the earlier papers which present all required formulae. The results of five-day forecasts are presented in Section 4. The interpolation schemes are first compared in terms of their conservation characteristics. The skill scores of the better schemes are then presented followed by a discussion of the characteristics of the precipitation fields. Finally, conclusions are presented in Section 5.

An important consideration for any numerical method is cost. The forecasts presented here are with an experimental code designed for generality rather than economy and provide no realistic estimate of overall efficiency. This important question will be addressed in future papers.

2. Model

The model used for the experiments described in this report is a diagnostic version of the NMC operational medium-range forecast model of May 1986 to August 1987 (Kanamitsu et al., 1988). This version has been labeled MRF86 (White, 1988). It is a global spectral model with rhomboidal 40 truncation in the horizontal and 18 unequally-spaced levels in the vertical. Conservative finite difference approximations are used in the vertical (Sela, 1982). Silhouette mountains are adopted with horizontal diffusion and sea surface temperatures adjusted to increase consistency with the orography. Physical parameterizations are based on the Geophysical Fluid Dynamics Laboratory (GFDL) E-2 physics package (Miyakoda and Sirutis, 1977) and include Kuo convection, shallow convection, grid-scale condensation and stability dependent vertical diffusion and surface exchange. Short wave radiation is based on Lacis and Hansen (1974) while long wave is based on Fels and Schwarzhopf (1975). The model assumes zonal average climatological cloudiness and has no diurnal variation.

Although the basic model domain consists of 18 layers, only the lowest 12 are used for the moisture variable (specific humidity) to save space. The upper boundary condition for specific humidity applied at the top of the twelfth level is that the vertical derivative vanishes. This standard version of the model was run to provide control forecasts for comparison with the semi-Lagrangian method and will be referred to as the spectral control model.

The moisture forecast equation can be written

$$\frac{\mathrm{d}q}{\mathrm{d}t} = S_{\mathrm{V}} + S_{\mathrm{A}},$$

where q denotes the specific humidity, S_{V} the source from the evaporation at the surface and the vertical redistribution by vertical diffusion, and S_{A} the source or sink associated with the adjustment physics (Kuo convective parameterization, shallow convection and grid scale precipitation). This adjustment physics is performed as a separate step in the control spectral model. The procedure can be described formally by

$$q^* = q^{\tau-1} + 2\Delta t\left(-V^{\tau}\cdot\nabla q^{\tau} - \dot{\sigma}^{\tau}\frac{\partial q^{\tau}}{\partial\sigma} + S_{\mathrm{V}}^{\tau}\right), \quad (1)$$

$$q^{\tau+1} = q^* + 2\Delta t\, S_{\mathrm{A}}^{\tau}. \quad (2)$$

The provisional value q^* is obtained via the conventional spectal transform method (Sela, 1982). The spectral forecast is reconstituted into grid values which are then modified by the adjustment processes S_{A} to give the final grid values $q^{\tau+1}$. These final values are spectrally truncated before the start of the next time step.

The experimental model is identical to the control spectral model except the moisture forecast is performed with a semi-Lagrangian algorithm and the moisture field is never spectrally truncated during the forecast. The semi-Lagrangian moisture forecast is performed with the S_{V} source term time split following Purnell (1976) in a second-order form and the adjustment term S_{A} fully time split as in the control spectral model. The experimental semi-Lagrangian version forecasts q from time $\tau - 1$ to time $\tau + 1$ to be consistent with the control model centered time differencing and with its adjustment physics. The moisture forecast is described by

$$q^* = L_{2\Delta t}(q^{\tau-1} + \Delta t\, S_{\mathrm{V}}^{\tau}) + \Delta t\, S_{\mathrm{V}}^{\tau}, \quad (3)$$

$$q^{\tau+1} = q^* + 2\Delta t\, S_{\mathrm{A}}^{\tau}. \quad (4)$$

Eqs. (3) and (4) are applied at the Gaussian gridpoints. The semi-Lagrangian operator $L_{2\Delta t}(\psi)$ represents the evaluation of the quantity ψ at the departure point via interpolation. The subscript $2\Delta t$ denotes the fact that the trajectories which provide the departure points are calculated over the $2\Delta t$ time interval. The horizontal trajectories are calculated following Williamson and Rasch (1989) using the mixed spherical-geodesic scheme poleward of 60° and the global spherical scheme equatorward of 60° with central wind components at time τ. Three iterations are performed with the first guess being the arrival point.

The forecast step (3) uses the evaporation and vertical diffusion (S_{V}^{τ}) exactly as calculated by the original control model code but this source term is not spectrally truncated. The semi-Lagrangian operator $L_{2\Delta t}$ is applied to $q^{\tau-1}$ after half the source has been added. The other half is added after the semi-Lagrangian operator is applied. The three-dimensional semi-Lagrangian advection is calculated by a further time splitting between the horizontal and vertical components. Thus, the advection operator alone can be written

$$\psi^{\tau+1} = L_{2\Delta t}(\psi^{\tau-1}) = A_{\sigma}[A_{\lambda,\phi}(\psi^{\tau-1})]. \quad (5)$$

The horizontal advection ($A_{\lambda,\phi}$) over $2\Delta t$ uses the tensor product form of interpolation and is performed first followed by the vertical (A_{σ}) over $2\Delta t$ (see Purnell (1976) or Williamson and Rasch (1989) for further discussion of time splitting). After completion of (3) the provisional q^* from the semi-Lagrangian step and a corresponding provisional T^* from the spectral algorithm are operated on by the adjustment physics to give the final $q^{\tau+1}$ and a corresponding $T^{\tau+1}$. The moisture field is never spectrally truncated, all other prognostic fields follow the usual spectral formalism of the control version. The time filter included in the control model is also applied to q in the semi-Lagrangian version. The only process not applied to the moisture in the semi-Lagrangian version that is included in the control version is the horizontal diffusion of moisture. The horizontal diffusion is applied to all other prognostic variables. Since the interpolation operators are somewhat diffusive, it was felt that an additional explicit diffusion term might not be needed. As in the control spectral model, moisture is only forecast in the lowest 12 levels with the top boundary condition that the vertical derivative vanish. The details of the implementation are presented at the end of the next section after the interpolation schemes are described.

3. Interpolation schemes

No one best scheme for moisture advection can be chosen based on the idealized test case studies of Rasch and Williamson (1989) and Williamson and Rasch (1989); rather many potential schemes can be eliminated leaving only the most promising to be evaluated in moisture advection itself. These most promising schemes are compared here.

The details of the interpolating schemes and nomenclature are presented in Williamson and Rasch (1989). We do not repeat them here. Instead we just summarize which combinations are evaluated in the current study. We consider the cubic Hermite interpolant and a rational cubic interpolant. Both forms require estimates of the derivatives at the ends of the interpolation intervals. We consider the cubic, Hyman and Akima derivative estimates. The formulas are summarized in the Appendix.

The cubic derivative estimate coupled with the Hermite cubic interpolant is included since it is equivalent to Lagrange cubic polynomial interpolation which has been used often for semi-Lagrangian models. The Hyman (1983) estimate is fourth-order on a smoothly varying grid mesh. The Akima (1970) estimate depends on the discrete curvature on the two sides of the point of application. For monotonic interpolators these estimates must be modified to satisfy the Necessary Condition for Monotonicity (NCM) for the rational cubic and the Sufficient Condition for Monotonicity (SCM) for the Hermite cubic. For C^0 continuity these abbreviations have a 0-suffix and for C^1 a 1-suffix. Particular combinations will be referred to by the form "interpolant/derivative-estimate/derivative-limiter" as, for example, rational/Hyman/NCM1 which denotes the rational cubic interpolant with the Hyman derivative estimate modified by the Necessary Condition for Monotonicity (C^1). If unmodified and therefore nonmonotonic derivative estimates are used the third component ("/derivative-limiter") is not included in the abbreviation. The formulae for the interpolants, derivative estimates and derivative limiters as used here are provided in Williamson and Rasch (1989) and summarized in the Appendix. For the vertical interpolation, the derivative estimate is taken to be zero at the top and bottom moisture levels and the moisture is assumed to be independent of σ outside these bounds and equal to the top or bottom grid value as appropriate. A noncentered Hyman (1983) estimate is used at the first point inside the top and bottom levels for the Hyman form. The Akima estimate at these points assumes a zero discrete slope outside the domain, consistent with the zero derivative boundary conditions. The cubic estimate uses that value calculated from the second interval for the first interval, and thus is C^1 at the first point inside the boundaries.

4. Forecast results

A series of five-day forecasts was made to evaluate the interpolation schemes for moisture advection. The initial data are from the NMC operational global analysis of 00 GMT 10 January 1987 initialized by the operational nonlinear normal mode initialization using the spectral control model. Thus, the initial moisture field has been spectrally truncated for all forecasts. For the semi-Lagrangian forecasts, the initial negative q values are set to a small positive number (1×10^{-5}), and no additional truncation takes place. In the spectral model, negative moisture values are set to the same small positive number (1×10^{-5}) whenever grid values are obtained from spectral coefficients.

4.1. Conservation

The semi-Lagrangian approach is not a priori conservative although in practice it may conserve extremely well and, in fact, if it is an accurate scheme it should conserve well. The importance of the nonconservation of moisture transport in a forced system such as the atmosphere could not be judged from the tests of Rasch and Williamson (1989) and Williamson and Rasch (1989). Therefore, we address this unanswered question first and analyze the conservation properties of the forecasts. Fig. 1 shows the global average moisture source and sink terms from a forecast with the Hermite/cubic/SCM0 combination. The

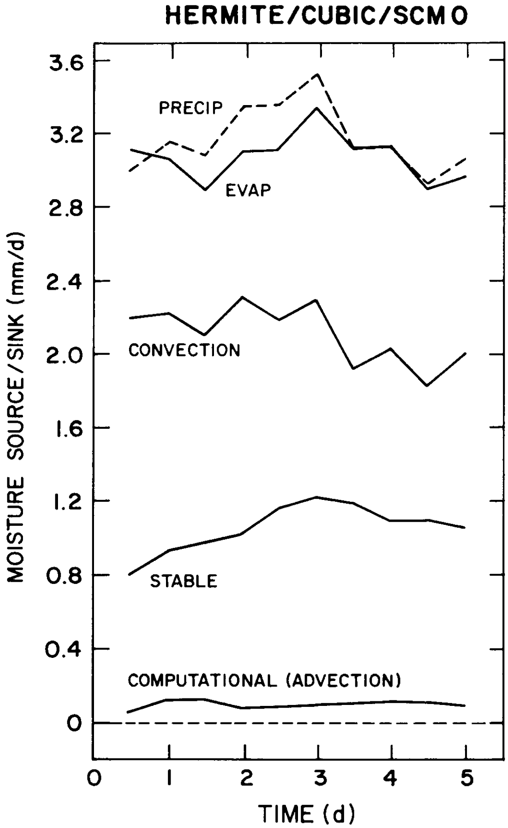

Fig. 1. Global average source and sink terms from semi-Lagrangian forecast with Hermite/cubic/SCM0 interpolant. Absolute values of precipitation (mm/day) are plotted. Values are accumulated over 12 h preceding plotted points.

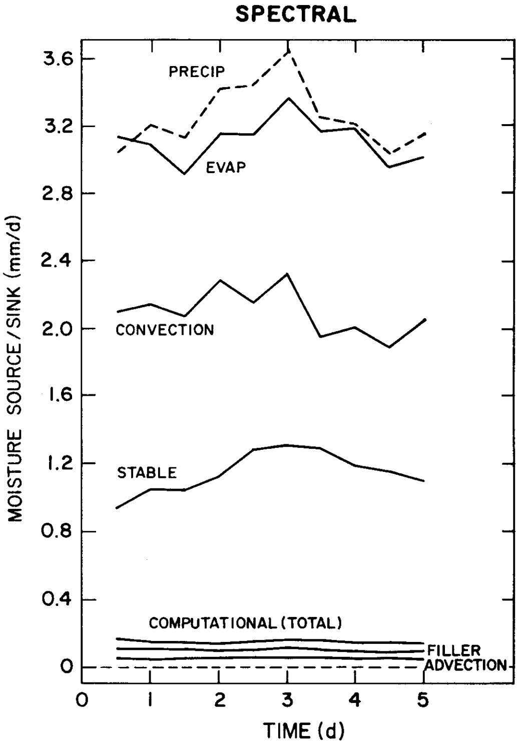

Fig. 2. Global average source and sink terms for spectral control forecast (see Fig. 1).

graph presents the absolute value of the average rate (mm/day) for the 12-h period preceding the plotted point. The total precipitation nearly balances the evaporation with very little spinup evident. The convective precipitation from the Kuo parameterization contributes about $\frac{2}{3}$ of the total and the large scale, stable condensation the remaining $\frac{1}{3}$. The nonconservation of the semi-Lagrangian advection results in a computational source which is about 10% of the smaller precipitation process or 3% of the total precipitation. This computational source does not appear to be unacceptable; however, to put it in proper perspective we also consider the spectral control forecast presented in Fig. 2.

The computational sources in the spectral control model can be divided into two parts. The first arises because the advective processes are not exactly conservative. The vertical advection finite difference approximations are conservative except for the top boundary condition. This condition, applied at the twelfth model layer is that the σ derivative of q is zero rather than that the flux is zero. (This same boundary condition was applied to the semi-Lagrangian model to be comparable and thus also contributes to the computational source in the semi-Lagrangian forecast.) This is the dominant computational advection source for the spectral control model and any source or sink from the horizontal spectral advection is negligible compared to it. The advective computational source from the spectral control forecast is the bottom curve in Fig. 2 (labeled advection). A larger computational source arises from filling negative moisture values following a spectral truncation of the specific humidity after advection is completed but before the adjustment physics is performed. In the spectral control forecast specific humidity values which are less than or equal to zero are set to 1.0×10^{-5}. This filling, which is performed before the adjustment physics is invoked, provides the computational source shown by the second curve from the bottom in Fig. 2 (labeled filler). It is twice as large as the advection source. The sum of the two or total computational source is shown by the third line from the bottom of Fig. 2. The total computational source in the spectral control is seen to be about 50% larger than the computational source in the Hermite/cubic/SCM0 semi-Lagrangian forecast. The filler itself in the spectral forecast is comparable to the computational source of the semi-Lagrangian. Thus the computational source of the semi-Lagrangian forecast is no worse than that of the spectral.

It is also interesting to compare the total precipitation and evaporation of the two forecasts. The evaporation from the spectral forecast is slightly larger (by ~1% or 0.04 mm/day) than that from the semi-Lagrangian while the total precipitation from the spectral is 0.04 to 0.10 mm/day larger. Most of that increase is due to the stable condensation. The convective precipitation is somewhat smaller in the spectral model for the first day, then the two schemes are comparable. We will return to the regional distribution of the precipitation later.

We next consider the conservation characteristics of other monotonic interpolants which were not eliminated in Williamson and Rasch (1989). The computational sources associated with the various interpolants coupled with the semi-Lagrangian advection are plotted in Fig. 3. The upper half graphs the Hermite interpolant with different derivative approximations. The stable precipitation from the Hermite/cubic/SCM0 of Fig. 1 is included for reference. The bottom curve of the top half is for the Hermite/cubic/SCM0 also copied from Fig. 1. The second curve from the bottom is for the Hermite/Hyman/SCM0 combination. This source is twice that of the Hermite/cubic/SCM0. The third curve in the top half is from the Hermite/Akima/SCM0 combination and is approximately twice that of the Hermite/Hyman/SCM0. The Hermite/Akima/SCM0 source is 35 to 40% of the stable precipitation, clearly too large to offer a viable scheme.

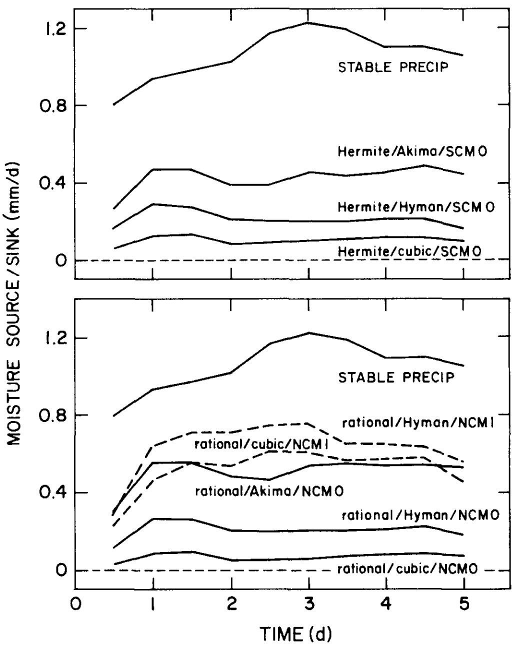

Fig. 3. Global average computational source terms from Hermite interpolant (upper half) and rational interpolant (lower half). Stable precipitation from Hermite/cubic/SCM0 interpolant (Fig. 1) is included for reference (mm/day).

The effect of this source is to increase the precipitation, primarily the stable component for the first half of the forecast, then both components, and to decrease the evaporation about equally. In addition the global average precipitable water increases. The Hermite/Hyman/SCM0 has a similar effect on the components, only with less magnitude. In this case, however, the convective precipitation is increased for the entire forecast, not just the last half.

The bottom half of Fig. 3 shows the global average source for the rational interpolant with the various monotonic derivative approximations. The stable precipitation from the Hermite/cubic/SCM0 is also copied to that half of the figure from Fig. 1 for reference. The rational/cubic/NCM0 is seen to be the best of this set with regard to conservation, and in fact, it is 20% better than the Hermite/cubic/SCM0. The computational source of the rational/Hyman/NCM0 is twice that of the rational/cubic/NCM0 and that of the rational/Akima/NCM0 is two and

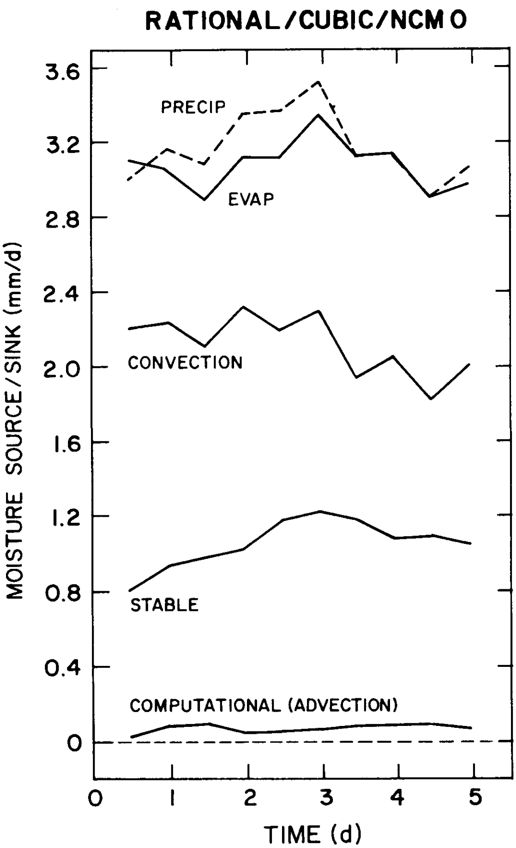

Fig. 4. Global average source and sink terms from semi-Lagrangian forecast with rational/cubic/NCM0 interpolant (see Fig. 1).

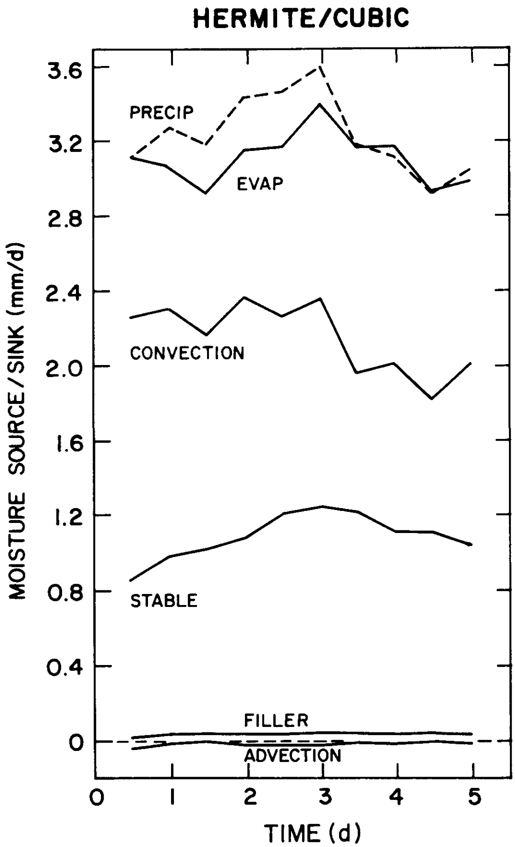

Fig. 5. Global average source and sink terms from semi-Lagrangian forecast with Hermite/cubic interpolant (see Fig. 1).

a half times that of the rational/Hyman/NCM0 or close to 50% of the stable precipitation of the spectral control. The computational sources of the C^1 continuous forms, rational/cubic/NCM1 and rational/Hyman/NCM1, are also 50% of the stable precipitation. The poor performance of the C^1 forms compared to the C^0 forms is somewhat surprising since in the earlier tests cited above which advect simpler structures the C^1 rational forms had better conservation characteristics than the corresponding C^0 forms. The C^1 forms are clearly unsuitable for the current applications as is the rational/Akima/NCM0. The rational/Hyman/NCM0 is perhaps marginally acceptable but at this point offers no advantages over the better rational/cubic/NCM0 combination.

Fig. 4 shows the global average evaporation, and precipitation for the rational/cubic/NCM0 case. Comparison with Fig. 1 shows that the global average characteristics of this combination are very similar to those of the Hermite/cubic/SCM0. The evaporation and precipitation of the other rational cases of Fig. 3 are affected by the computational source. The rational/Hyman/NCM0, which was the second best as far as the computational source is concerned, has a slight decrease in evaporation, slight increase in stable precipitation and a slight increase in precipitable water compared to the rational/cubic/NCM0 (or Hermite/cubic/SCM0 or spectral for that matter). The other three cases shown at the bottom of Fig. 3 are significantly worse. The rational/cubic/NCM1, rational/Hyman/NCM1 and rational/Akima/NCM0 all have decreased evaporation,

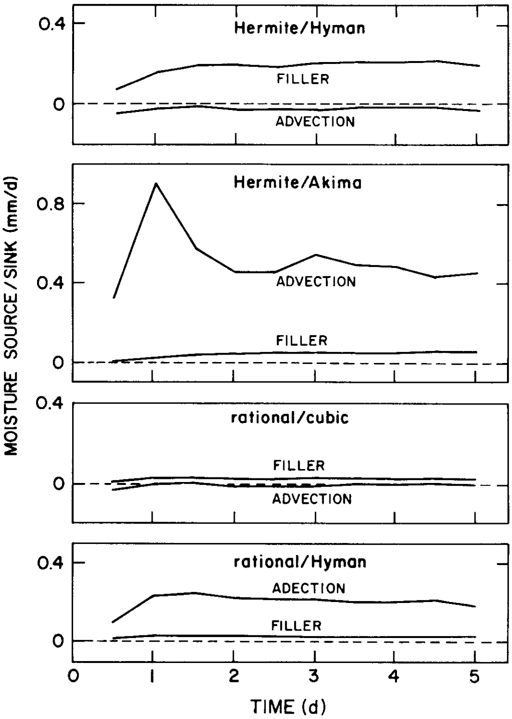

Fig. 6. Global average computational source and sink terms from semi-Lagrangian forecasts with various nonmonotonic interpolants (mm/day).

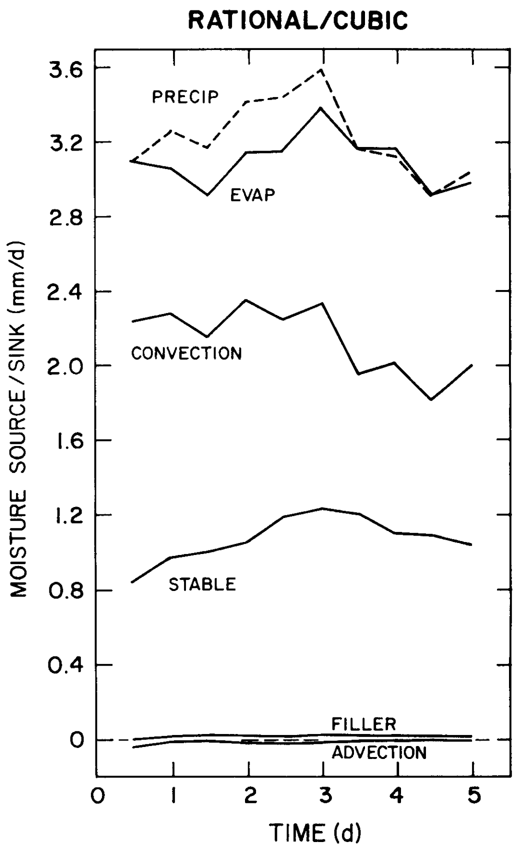

Fig. 7. Global average source and sink terms from semi-Lagrangian forecasts with rational/cubic interpolant (see Fig. 1).

increased stable and convective precipitation and increased precipitable water. Of these three the rational/Akima/NCM0 has the largest changes in all these quantities even though the computational sources of the NCM1 forms tend to be larger.

It is also of interest to consider forecasts with unconstrained or nonmonotonic interpolants since such forms have been commonly used for semi-Lagrangian models. Fig. 5 shows the global average terms for the Hermite/cubic combination which is equivalent to Lagrange cubic polynomial interpolation. This is essentially the scheme used by Ritchie (1985) for his tests of semi-Lagrange moisture transport in the DRPN regional finite-element model. Since the scheme is not monotonic some negative values may occur after the advection step, which as in the spectral model are set to 1×10^{-5} before the adjustment physics is invoked. This filler provides a computational source of moisture and is included in Fig. 5. It is seen to be smaller than any of the computational sources of the other schemes examined so far. There is also a source or in this case a sink of moisture due to the advection itself not being a priori conservative. This is also shown in Fig. 5. It is also very small and about the same size, but opposite sign, as the filler term. In this case these two computational sources tend to partially cancel.

The stable precipitation from the Hermite/cubic case is less than that from the spectral and more than that from the Hermite/cubic/SCM0. The convective precipitation from the Hermite/cubic exceeds that of the spectral and Hermite/cubic/SCM0 for the first three days then remains comparable. The evaporation in all cases is fairly similar.

Fig. 6 shows the global average of the filler and advective sources for the other unlimited inter-

Table 1. *Various northern hemisphere skill scores for forecasts with spectral control model and semi-Lagrangian moisture transport version with Hermite/cubic and Hermite/cubic/SCM0 interpolants*

	1000 mb			500 mb		
Day	Spectral	Hermite/cubic	Hermite/cubic/SCM0	Spectral	Hermite/cubic	Hermite/cubic/SCM0
			Anomaly correlation			
1	0.9637	0.9633	0.9635	0.9814	0.9814	0.9812
2	0.9030	0.9011	0.8980	0.9305	0.9282	0.9270
3	0.7501	0.7484	0.7462	0.8292	0.8295	0.8268
4	0.5011	0.5036	0.5048	0.6158	0.6255	0.6230
5	0.3842	0.3810	0.3865	0.4689	0.4713	0.4673
			RMS error			
1	26.78	27.04	26.98	25.03	24.98	25.13
2	43.15	43.46	44.17	47.92	48.68	49.11
3	66.52	66.91	67.25	73.40	73.45	74.13
4	88.90	88.92	88.87	103.58	102.85	103.38
5	88.62	89.18	89.14	117.38	118.08	118.98
			Mean error			
1	3.01	3.56	3.61	−3.34	−3.43	−3.99
2	1.70	2.28	2.16	−7.17	−7.62	−8.45
3	3.11	4.16	4.21	−7.13	−7.45	−8.71
4	−0.59	1.30	1.07	−17.49	−18.22	−19.70
5	−8.55	−7.01	−7.17	−31.17	−32.60	−33.58

polants. The Hermite/Hyman has a very small advective sink but creates fairly large negative values or regions which require a rather hefty filler as large as 20% of the stable precipitation of the Hermite/cubic. On the other hand, the Hermite/Akima produces relatively small negative values but conserves poorly resulting in a fairly large computational source from the advection, being close to 50% of the stable precipitation in the Hermite/cubic. The rational/cubic appears to be slightly better than the Hermite/cubic. The negative amounts and therefore filler are comparable to that of the Hermite/cubic, but the advective sink is somewhat smaller, and for the latter part of the forecast cannot be distinguished on the graph from the zero line. In fact it oscillates in sign between being a small sink and source during the last two days of the forecast. The rational/Hyman also requires a relatively small filler but has a not insignificant advective source comparable to the filler of the Hermite/Hyman.

Fig. 7 shows the global average precipitation and evaporation for the rational/cubic case. They are seen to be almost identical to the corresponding terms of the Hermite/cubic. Also, recall that their corresponding monotonic forms, Hermite/cubic/SCM0 and rational/cubic/NCM0, were also almost identical to each other. The small differences between these two pairs are due to the occasional modification of the derivative estimates to ensure monotonicity. Of all the schemes considered earlier in Rasch and Williamson (1989) and Williamson and Rasch (1989), only these four (Hermite/cubic, rational/cubic, Hermite/cubic/SCM0 and rational/cubic/NCM0) seem suitable for global moisture advection, at least at this R40 resolution. Only the latter two are monotonic or shape preserving.

4.2. *Skill scores*

Table 1 lists some selected skill scores calculated over the Northern Hemisphere for the forecasts from the spectral model and from the semi-Lagrangian moisture versions using the

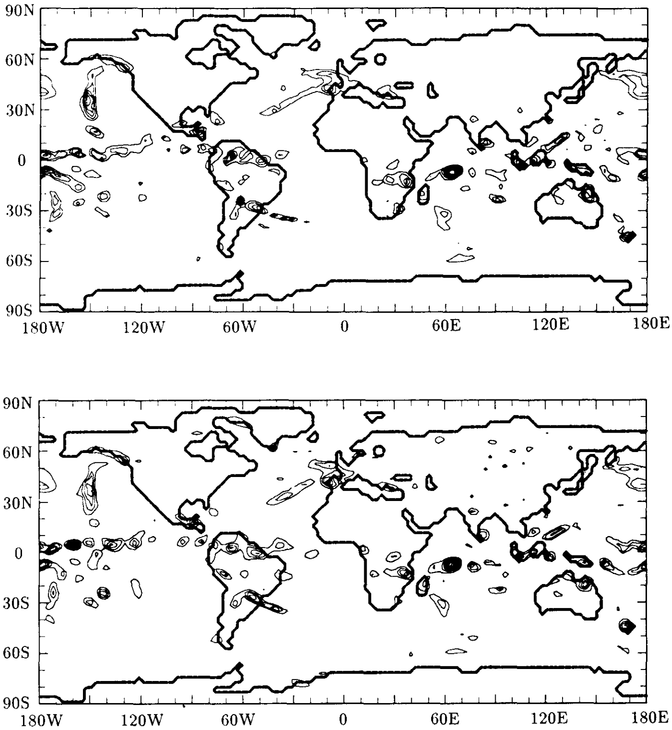

Fig. 8. Twenty-four hour average precipitation for days 4–5 for semi-Lagrangian forecast with Hermite/cubic/SCM0 interpolant (top) and spectral control forecast (bottom). Contour interval is 10 mm/day.

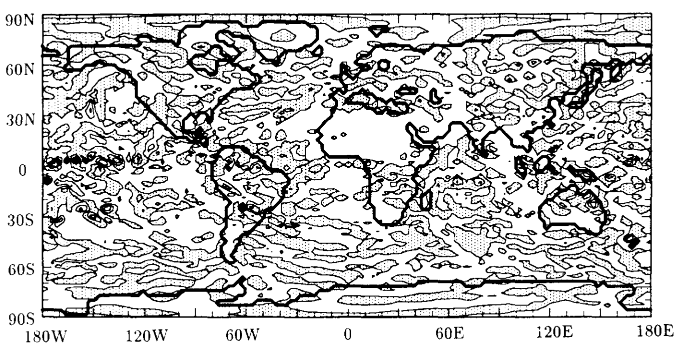

Fig. 9. Difference of 24-h average precipitation for days 4–5 of semi-Lagrangian forecast with Hermite/cubic/SCM0 interpolant minus spectral forecast. Contour interval is 10 mm/day.

Hermite/cubic and Hermite/cubic/SCM0 interpolants. Recall that the Hermite/cubic interpolant is equivalent to Lagrange cubic polynomial interpolation which has often been used in semi-Lagrangian models. The obvious conclusion to be drawn from this table is that there is little if any difference in the large-scale skill of these forecasts as determined by the traditional global measures. Given that these scores are calculated for one forecast of one case for each of the schemes, it would be impossible to conclude that they are significantly different.

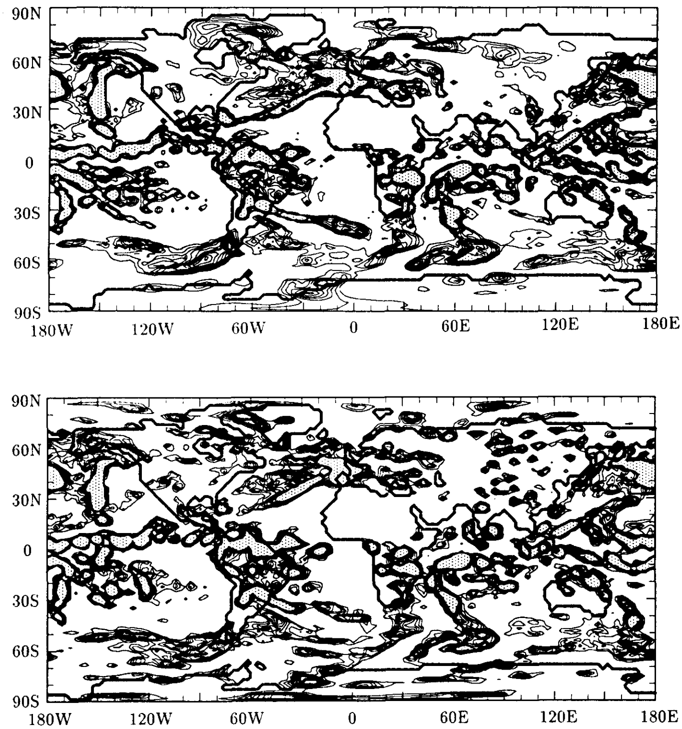

Fig. 10. Twenty-four hour average precipitation for days 4–5 for semi-Lagrangian forecast with Hermite/cubic/SCM0 interpolant (top) and spectral control forecast (bottom). Contour interval is 1.0 mm/day. Areas greater than 10 mm/day are stippled.

4.3. Precipitation

Fig. 8 shows the 24-h average precipitation from day 4 to day 5 for the forecast with Hermite/cubic/SCM0 (top) and the spectral control (bottom). Even after 4 days the precipitation patterns are remarkably similar. The major cells occur in the same regions in both forecasts, although details of the cells are somewhat different. Fig. 9 shows the difference of the semi-Lagrangian minus the spectral precipitation fields of Fig. 8. Negative (stippled) values occur where the precipitation of the spectral model exceeds that of the semi-Lagrangian. This difference map indicates that the overall characteristics of the precipitation fields are very different even though the major cells shown in Fig. 8 are very similar. The difference map indicates that one of the models, presumably the spectral, produces a precipitation field strongly modulated by the spectral representation. This is most noticeable in the Southern Hemisphere south of 45°S.

The precipitation caused by a modulation of the moisture field due to the truncation in the spectral model is seen much more clearly in Fig. 10. This figure presents the same precipitation fields shown in Fig. 8 but with one-tenth the contour interval. The regions within the first contour of Fig. 8 are stippled in Fig. 10. Small amounts of precipitation caused by spectral ringing are clearly evident in the Southern Hemisphere south of 45°S in the spectral forecast (bottom panel). The semi-Lagrangian forecast shows larger, more coherent regions of precipitation which are more likely to be physically based, or at least consistent with the model's parameterization schemes without modulation by the numerics. The spectral model also exhibits more noise in the regions where the precipitation tends to be more coherent. Compare, for example, the large area of precipitation centered on 60°S between 150°W and 75°W. This area is included in an enlargement in Fig. 11 in which the different structures are more apparent. The

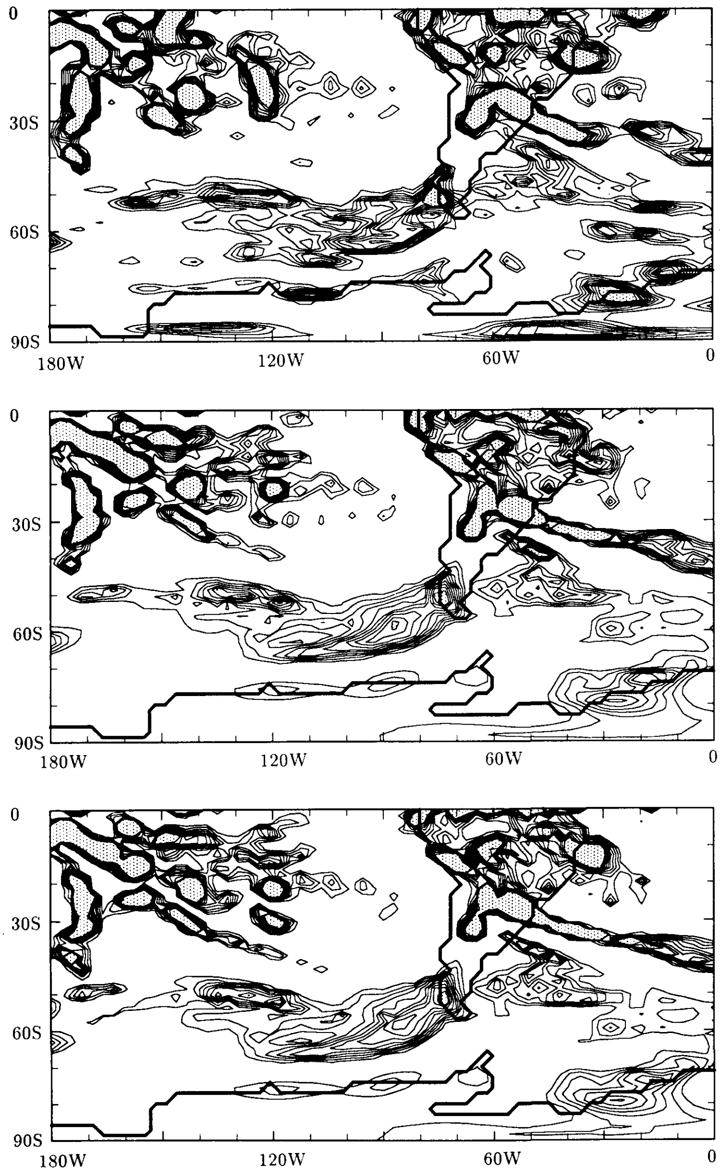

Fig. 11. Enlargement. of precipitation fields in Fig. 10. Note that fields are reversed from those in Fig. 10, spectral control forecast (top), semi-Lagrangian forecast with Hermite/cubic/SCM0 interpolant (middle) and with Hermite/cubic interpolant (bottom). Contour interval is 1.0 mm/day with areas greater than 10 mm/day stippled.

regions of small amounts of precipitation which are likely to be physically based are strongly modulated by the spectral truncation inherent in the spectral model. The cold areas of the Northern Hemisphere also demonstrate a significant difference in the characteristics of the light precipitation between the two approaches (Fig. 10). In Siberia, for example, the semi-Lagrangian shows very little precipitation while the spectral produces a very noisy, grid-scale precipitation

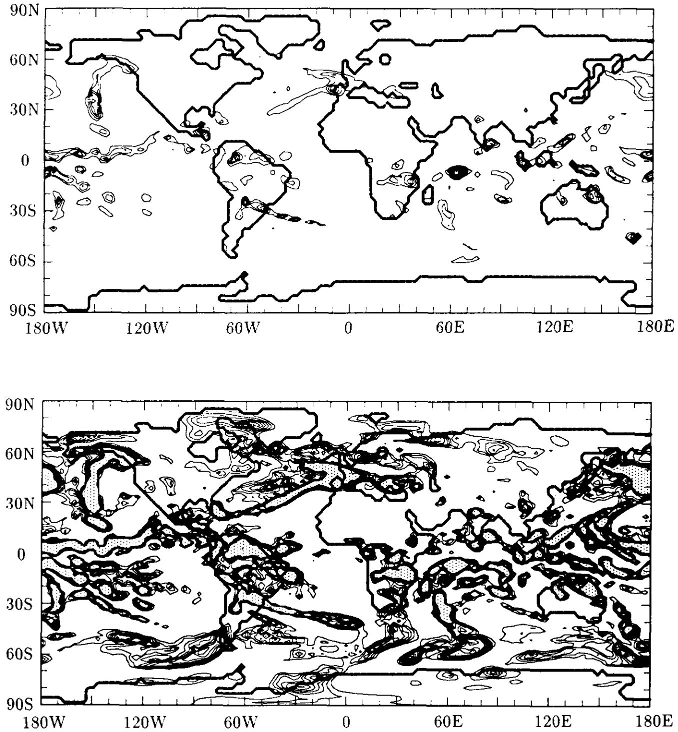

Fig. 12. Twenty-four hour average precipitation for days 4–5 for semi-Lagrangian forecast with Hermite/cubic interpolant. Top: contour interval is 10 mm/day. Bottom: contour interval is 1 mm/day with areas greater than 10 mm/day stippled.

field. Similar differences occur in Fig. 10 over northern North America.

This spurious precipitation in the spectral model has little direct effect on the large-scale forecasts with this model as demonstrated earlier by the skill scores. The precipitation amounts are very small and thus the direct heating via release of latent heat has minimal effect in forcing the atmosphere. Noisy spurious precipitation may have a significant effect on model forecasts in the future when interactive clouds are introduced. The forecasts discussed here used specified zonal average clouds for the radiation parameterization. If clouds are diagnosed from model state variables and depend on the characteristics of the precipitation as well, significant spurious heating could be introduced via the interaction of the clouds with the radiation.

Fig. 12 shows the precipitation from the semi-Lagrangian forecast with the Hermite/cubic interpolant. The top panel uses the contour interval of 10 mm/day and is comparable to Fig. 8 while the bottom uses the contour interval of 1 mm/day with areas greater than 10 mm/day stippled and is comparable to Fig. 10. An enlargement is also included as the bottom panel in Fig. 11. Comparison of Fig. 12 with Figs. 8 and 10 shows that the nonmonotonic interpolant (Hermite/cubic) produces precipitation remarkably like that of the monotonic interpolant (Hermite/cubic/SCM0), even for the small amounts of 1 mm/day. The constraint on the derivative estimates to ensure monotonicity is only invoked occasionally and has a small effect on the precipitation. The precipitation fields from the rational/cubic and rational/cubic/NCM0 also look remarkably like those of the Hermite/cubic/SCM0 and are not shown here. These four interpolants in the semi-Lagrangian forecasts produce very similar precipitation fields which are very different in character from those of the spectral model.

5. Conclusions

The moisture transport scheme in the NMC spectral model was replaced with a semi-Lagrangian scheme using shape preserving interpolation as proposed by Rasch and Williamson (1989) and Williamson and Rasch (1989). Of the multitude of shape preserving interpolants that have been introduced in the literature, many were eliminated from consideration for moisture transport in the two studies cited above. Those studies used simple test beds to compare schemes and could not safely provide a basis for choosing one best scheme for moisture transport. Therefore, the remaining contenders were first examined in the NMC model in terms of their moisture conservation characteristics during five-day forecasts. Many of these schemes were found to be unsuitable for moisture transport because their spurious moisture source associated with the semi-Lagrangian advection was a significant fraction of the precipitation, at least at the R40 resolution considered here. There were, however, several schemes that behaved very well, in fact better than the spectral if one compared their spurious sources to the negative mixing ratios introduced by the spectral method. These schemes were the Hermite/cubic/SCM0, rational/cubic/NCM0, Hermite/cubic and rational/cubic. The first two are monotonic, while the second two are not shape preserving at all. Nevertheless these second two were considered since the Hermite/cubic is equivalent to Lagrange cubic polynomial interpolation, which has been widely used in semi-Lagrangian models, and the rational/cubic was just slightly better than the Hermite/cubic. The two monotonic interpolators produced global average precipitation and evaporation values which were almost identical. Similarly, the global average values from the two nonmonotonic interpolators were also almost identical, but slightly different from those of the monotonic forms or spectral model. The differences between the global average produced by these three classes were small enough that one could not pass judgment as to the relative merits of the schemes from this measure alone.

The traditional global skill scores, namely anomaly correlation and rms, were calculated for the forecasts. No significant difference in these scores could be identified indicating that all forecasts were equally good in these average terms.

Finally, the precipitation fields were examined. The main precipitation cells produced by the various schemes were remarkably similar indicating that they perform equally well on the principal precipitation events. The overall patterns of the regions of light precipitation were very different, however, between the spectral and semi-Lagrangian. The precipitation fields from the four semi-Lagrangian forecasts were very similar. The spectral model produced precipitation which could be attributed to the spectral truncation. This spurious precipitation was particularly evident in the Southern Hemisphere polar regions south of 45°S and over the cold land masses in the Northern Hemisphere. The semi-Lagrangian method eliminated this spurious precipitation. Although the direct heating from release of latent heat of the spurious precipitation seems to have little detrimental effect on the forecast with the current NMC model (other than the spurious precipitation itself), the spurious precipitation may become detrimental in future versions. The current version uses specified, zonal average clouds in the radiative parameterization. When interactive clouds are introduced, which depend on the state variables and precipitation characteristics, spurious radiative heating will arise in the spectral method. This problem is eliminated by semi-Lagrangian transport of moisture.

6. Acknowledgements

This study was done in parallel with a similar study with P. Rasch involving climate simulations with the NCAR Community Climate Model to be presented elsewhere. I would like to thank Phil for many stimulating discussions. I would also like to thank the staff members of NMC for their help and hospitality during and after my visit. R. Balgovind and B. Katz of Centel Federal Services Corporation provided essential programming assistance at NMC and B. Eaton provided similar assistance at NCAR. E. Boettner provided editorial assistance and produced the final manuscript.

7. Appendix

Interpolation forms

For interpolation on the interval $x_i \leqslant x \leqslant x_{i+1}$

$$p_i = P_i(\theta)/Q_i(\theta), \tag{A1}$$

where

$$P_i(\theta) = f_{i+1}\theta^3 + (r_i f_{i+1} - h_i d_{i+1})\theta^2(1-\theta) + (r_i f_i + h_i d_i)\theta(1-\theta)^2 + f_i(1-\theta)^3, \tag{A2}$$

$$Q_i(\theta) = 1 + (r_i - 3)\theta(1-\theta), \tag{A3}$$

$$h_i = x_{i+1} - x_i, \tag{A4}$$

$$\theta = (x - x_i)/h_i, \tag{A5}$$

and f_i and d_i denote the datum and an estimate of the derivative at x_i, respectively.

For the Hermite cubic polynomial interpolant

$$r_i = 3. \tag{A6}$$

For the rational cubic interpolant

$$r_i = 1 + \frac{c_{i+1}}{c_i} + \frac{c_i}{c_{i+1}}, \tag{A7}$$

where

$$c_i = \Delta_i - d_i, \tag{A8}$$

$$c_{i+1} = d_{i+1} - \Delta_i, \tag{A9}$$

$$\Delta_i = \frac{(f_{i+1} - f_i)}{(x_{i+1} - x_i)}. \tag{A10}$$

Derivative estimates

Cubic:

$$d_i = \begin{cases} f[x_i, x_{i-1}] + (x_i - x_{i-1}) f[x_{i+1}, x_i, x_{i-1}] \\ \quad + (x_i - x_{i-1})(x_i - x_{i+1}) \\ \quad \times f[x_{i+2}, x_{i+1}, x_i, x_{i-1}] \\ \quad \text{for interpolation in } (x_i, x_{i+1}), \\ f[x_{i-1}, x_{i-2}] + \{(x_i - x_{i-1}) + (x_i - x_{i-2})\} \\ \quad \times f[x_i, x_{i-1}, x_{i-2}] \\ \quad + (x_i - x_{i-2})(x_i - x_{i-1}) \\ \quad \times f[x_{i+1}, x_i, x_{i-1}, x_{i-2}] \\ \quad \text{for interpolation in } (x_{i-1}, x_i), \end{cases} \tag{A11}$$

using the normal divided difference notation

$$f[x_2, x_1] = (f(x_2) - f(x_1))/(x_2 - x_1),$$
$$f[x_n, x_{n-1}, \ldots, x_1] = (f[x_n, x_{n-1}, \ldots, x_2] - f[x_{n-1}, x_{n-2}, \ldots, x_1])/(x_n - x_1). \tag{A12}$$

Hyman:

$$d_i = \frac{-f_{i+2} + 8f_{i+1} - 8f_{i-1} + f_{i-2}}{-x_{i+2} + 8x_{i+1} - 8x_{i-1} + x_{i-2}}. \tag{A13}$$

Akima:

$$d_i = \begin{cases} \dfrac{\alpha\Delta_{i-1} + \beta\Delta_i}{\alpha + \beta} & \alpha + \beta \neq 0 \\ \dfrac{\Delta_{i-1} + \Delta_i}{2} & \alpha + \beta = 0, \end{cases} \tag{A14}$$

where

$$\alpha = |\Delta_{i+1} - \Delta_i|,$$
$$\beta = |\Delta_{i-1} - \Delta_{i-2}|. \tag{A15}$$

Shape preserving derivative constraints

Necessary condition for monotonicity, C^0

$$\begin{array}{ll} \operatorname{sgn}(d_i) = \operatorname{sgn}(\Delta_i) = \operatorname{sgn}(d_{i+1}), & \Delta_i \neq 0, \\ d_i = d_{i+1} = 0, & \Delta_i = 0. \end{array} \quad \text{(NCM0)} \tag{A16}$$

Necessary condition for monotonicity, C^1

$$\begin{array}{ll} \operatorname{sgn}(\Delta_{i-1}) = \operatorname{sgn}(d_i) = \operatorname{sgn}(\Delta_i), & \Delta_{i-1}\Delta_i > 0, \\ d_i = 0, & \Delta_{i-1}\Delta_i \leqslant 0. \end{array} \quad \text{(NCM1)} \tag{A17}$$

Sufficient condition for monotonicity

$$0 \leqslant \alpha \leqslant 3 \quad \text{and} \quad 0 \leqslant \beta \leqslant 3, \tag{A18}$$

where

$$\alpha = d_i/\Delta_i, \tag{A19}$$

$$\beta = d_{i+1}/\Delta_i. \tag{A20}$$

The C^0 and C^1 forms (denoted SCM0 and SCM1) are obtained by bounding the derivatives based on Δ of the internal being interpolated or by the Δ of the two adjacent intervals simultaneously, respectively.

REFERENCES

Akima, H. 1970. A new method of interpolation and smooth curve fitting based on local procedures. *J. Assoc. Comput. Mach. 17*, 589–602.

Fels, S. B. and Schwarzhopf, M. D. 1975. The simplified exchange approximation: A new method for radiative transfer calculations. *J. Atmos. Sci. 32*, 1475–1488.

Hyman, J. M. 1983. Accurate Monotonicity preserving cubic interpolations. *SIAM J. Sci. Stat. Comput. 4*, 645–654.

Kanamitsu, M., Katz, B. and Dey, C. 1988. Utilization of predicted surface fields in the NMC data assimilation system. *Preprints, 8th Conf. on Numerical Weather Prediction, 22–26 February, 1988*. Baltimore, Md., 220–223.

Lacis, A. A. and Hansen, J. E. 1974. A parameterization for the absorption of solar radiation in the earth's atmosphere. *J. Atmos. Sci. 31*, 118–133.

Mahlman, J. D. and Sinclair, R. W. 1977. Tests of various numerical algorithms applied to a simple trace constituent air transport problem. *Fate of pollutants in the air and water environments,* vol 8, Part 1 (ed. I. H. Suffet). N.Y.: John Wiley, 223–252.

Miyakoda, K. and Sirutis, J. 1977. Comparative integration of global models with various parameterized processes of sub-grid scale vertical transports: Description of the parameterization. *Bietr. Phys. Atmos. 50*, 445–487.

Purnell, D. K. 1976. Solution of the advective equation by upstream interpolation with a cubic spline. *Mon. Wea. Rev. 104*, 42–48.

Rasch, P. J. and Williamson, D. L. 1989. On shape preserving interpolation and semi-Lagrangian transport. *SIAM J. Sci. Stat. Comput.*, in press.

Ritchie, H. 1985. Application of a semi-Lagrangian intergration scheme to the moisture equation in a regional forecast model. *Mon. Wea. Rev. 113*, 424–435.

Royer, J. F. 1986. Correction of negative mixing ratios in spectral models by global horizontal borrowing. *Mon. Wea. Rev. 114*, 1406–1410.

Sela, J. G. 1982. The NMC spectral model. *NOAA Tech. Rept. NWS 30* (available from National Technical Information Service, 5285 Port Royal Road, Springfield, VA 22161), 36 pp.

White, G. H. 1988. Systematic performance of NMC medium-range forecasts 1985–88. *Preprints, 8th Conf. on Numerical Weather Prediction, 22–26 February, 1988*. Baltimore, Md., 466–471.

Williamson, D. L. and Rasch, P. J. 1989. Two-dimensional semi-Lagrangian transport with shape preserving interpolation. *Mon. Wea. Rev. 117*, 102–129.